

FULL TITLE
*ASP Conference Series, Vol. **VOLUME**, **YEAR OF PUBLICATION***
 NAMES OF EDITORS

Theory of Outflows in Cataclysmic Variables

D. Proga

JILA, University of Colorado, Boulder CO 80309, USA
Present address: Department of Astrophysical Sciences, Princeton
University, Peyton Hall, Princeton NJ 08544, USA

Abstract. We review the main results from line-driven (LD) models of winds from accretion disks in cataclysmic variables (CVs). We consider LD disk wind models in the hydrodynamic (HD) and magnetohydrodynamic (MHD limits. We discuss the basic physical conditions needed for a disk wind to exist and the conditions for the wind to be steady or unsteady. We also discuss how the line-driven (LD) wind structures revealed in numerical simulations relate to observations. In particular, we present synthetic line profiles predicted by the LD wind models and compare them with observations. Our main conclusion is that, despite some problems, line-driving alone is the most plausible mechanism for driving the CV winds. This conclusion is related to two facts: 1) LD wind models are likely the best studied wind models, analytically and numerically, and 2) it is most likely that the predictive power of the LD wind models is much higher than of any other wind model so far. Preliminary results from LD-MHD wind models confirm that magnetic driving is likely an important element of the wind dynamics. However, magnetic driving does not seem to be necessary to produce a CV wind. The most important issues which need to be addressed by future dynamical models, regardless of driving mechanism, are the effects of the position-dependent photoionization and the dynamical effects in three dimensions.

1. Introduction

Winds in cataclysmic variables (CVs) exemplify very well a phenomenon of accretion disks being accompanied by mass outflows. Other systems where this phenomenon occurs are active galactic nuclei (AGN) and young stellar objects (YSOs). In the case of CVs, key evidence for outflows comes from P-Cygni profiles of strong UV lines such as C IV λ 1549. However, the evidence for the winds is not limited just to the strong UV lines Long & Knigge (2002). Understanding the winds in CVs is important on its own right and because they have been the best observed outflows from compact objects and promise to provide us with insights into all disk outflows. The interpretation of data is usually based on fitting observed profiles to synthetic profiles calculated from kinematic models (e.g., Mauche & Raymond 1987; Drew 1987; Shlosman & Vitello 1993; Knigge, Woods, & Drew 1995; Long & Knigge 2002). We refer a reader to Froning (2004, this volume) for a review of the observations and interpretations of CV winds.

Magnetic fields, the radiation force and thermal expansion have been suggested as mechanisms that can drive disk winds. These three mechanisms have

been studied extensively using analytic as well as numerical methods. As a result of these studies, theoretical models have been developed that allow us to estimate under what physical conditions each of these mechanisms is efficient in launching, accelerating and collimating disk outflows. Here we will focus on models of radiation-driven disk winds (section 2) and a hybrid model in which both radiation and magnetic driving is considered (section 3).

2. LD HD Models

More than three decades of studies of winds in hot stars provide us with a very good understanding of how line-driving produces powerful high velocity winds (e.g., Castor, Abbott & Klein 1975, hereafter CAK; Friend & Abbott 1986; Pauldrach, Puls, & Kudritzki 1987). The key element of the CAK model is that the momentum is extracted most efficiently from the radiation field via line opacity. The Eddington limit, $L_{\text{Edd}} = 4\pi cGM/\sigma_e$, is the maximum luminosity a spherical object of mass M may achieve before the radiation pressure mediated by photons scattering off free electrons becomes so large as to drive off the object's atmosphere and envelope. It is commonly the case that the effective cross section for photon scattering is greatly increased by the presence of Doppler-shifting bound-bound transitions. CAK showed that the radiation force due to lines, $F^{\text{rad},l}$ can be stronger than the radiation force due to electron-scattering, $F^{\text{rad},e}$ by up to several orders of magnitude (i.e., $F^{\text{rad},l}/F^{\text{rad},e} < M_{\text{max}} \approx 2000$). Thus even a star that radiates at around 0.05% (i.e., $1/M_{\text{max}}$) of its Eddington limit can have a strong wind.

Early models of radiation-driven disk winds have applied assumptions that either restrict the flow geometry or require the flow to be time-independent [e.g. Vitello & Shlosman (1988) and a model for AGN wind by Murray et al. (1995)]. Recently numerical models of 2.5-D, time-dependent radiation driven disk winds have been constructed for application to, in the first instance, CV disk winds (e.g., Pereyra, Kallman, & Blödorn 1997; Proga, Stone, & Drew 1998, hereafter PSD 98; Proga, Stone, & Drew 1999, hereafter PSD 99; Proga 1999). In particular, PSD 98 adopted numerical techniques to integrate the coupled HD and radiation transfer equations in order to study the multidimensional and time-dependent character of line-driven (LD) disk winds from first principles. For the HD equations, they used the well-tested ZEUS code (Stone & Norman 1992) extended by the addition of a term in the equation of motion which accounts for the radiation force due to spectral lines of the form

$$F^{\text{rad},l} = \int_{\Sigma} \left(\frac{\sigma_e d\mathcal{F}}{c} \right) M(t). \quad (1)$$

The term in brackets is the electron scattering radiation force ($F^{\text{rad},e}$) and M , the force multiplier, is the increase in opacity due to spectral lines. The integration is over all visible radiating surfaces (Σ). Note that $d\mathcal{F}$ contains the total frequency-integrated intensity emitted at a given location. PSD 98 adopted the simple form for M which still underpins much modeling of OB star winds, i.e. $M = kt^{-\alpha}$, where t is proportional to the local density divided by the local velocity gradient, and k and α are constants (CAK). The maximum values of M , M_{max} determines the actual luminosity limit (the effective Eddington limit, $L_{\text{E}}/M_{\text{max}}$) for which the radiation pressure mediated by photons becomes large

enough to drive off the object's atmosphere and envelope. Note that integration over angle of a nonlinear function of the velocity gradient tensor and the radiation flux is required to evaluate equation (1); Proga, Stone, & Drew took great care in the numerical evaluation of these integrals by adopting angle-adaptive quadrature methods. PSD 98's formalism allows the radiation from the central accreting star to be included both as a direct contributor to the radiation force and as an indirect component via disk irradiation and reemission. To spatially resolve the flow, we used a non-uniform (up to 200×200) grid in which the subsonic acceleration zone near the disk or stellar surface is well sampled.

The primary outcome of the numerical studies is the confirmation that line driving can produce a supersonic, biconical wind from an accretion disk in CVs.

PSD 98 explored the impact upon the mass-loss rate, \dot{M}_w and outflow geometry caused by varying the system luminosity and the radiation field geometry. In their study, the system luminosity, L was defined as the sum of the disk luminosity and the central star luminosity, L_D and L_* , respectively (i.e., $L = L_D + L_* = (1 + x)L_D$, where $x = L_*/L_D$). A striking outcome was that winds driven from, and illuminated solely by, an accretion disk yield complex, unsteady outflow (see the top panels in Figure 1). In this case, time-independent quantities can be determined only after averaging over several flow timescales. On the other hand, if winds are illuminated by radiation mainly from the central object, then the disk yields steady outflow (see the bottom panels on Figure 1). PSD 98 also found that \dot{M}_w is a strong function of the total luminosity, while the outflow geometry is determined by the geometry of the radiation field. For high system luminosities, the disk mass-loss rate scales with the luminosity in a way similar to stellar mass loss (e.g., compare the crosses and the solid-line curve on Figure 2). As the system luminosity decreases below a critical value (the Eddington factor, $\Gamma \equiv L/L_{\text{Edd}}$ about twice $1/M_{\text{max}}$) the mass-loss rate decreases quickly to zero.

The simulations also showed that regardless of the radiation geometry, the two-dimensional structure of the wind consists of a dense, slow outflow that is bounded on the polar side by a high-velocity stream (respectively 'slow wind' and 'fast stream', for short; see e.g., Figure 1). Matter is fed into the fast stream from within a few central object radii. In other words, the mass-loss rate per unit area decreases sharply with radius. The terminal velocity of the stream is similar to that of the terminal velocity of a corresponding spherical stellar wind, i.e., $v_\infty \sim$ a few v_{esc} , where v_{esc} is the escape velocity from the photosphere. Thus the difference in geometry changes the wind geometry and time behavior but has less effect on M_w and v_∞ .

PSD 99 applied a more accurate treatment of the line force than PSD 98 by including all the terms in the velocity gradient tensor. Qualitative features of the new models are very similar to those calculated by PSD 98. In particular, the more accurate calculations showed that models which displayed unsteady behavior in PSD 98 are also unsteady with the new method, and gross properties of the winds, such as mass-loss rate and characteristic velocity are not changed by the more accurate approach. The largest change caused by the new method is in the disk-wind opening angle: winds driven only by the disk radiation are more polar with the new method while winds driven by the disk and central object radiation are typically more equatorial.

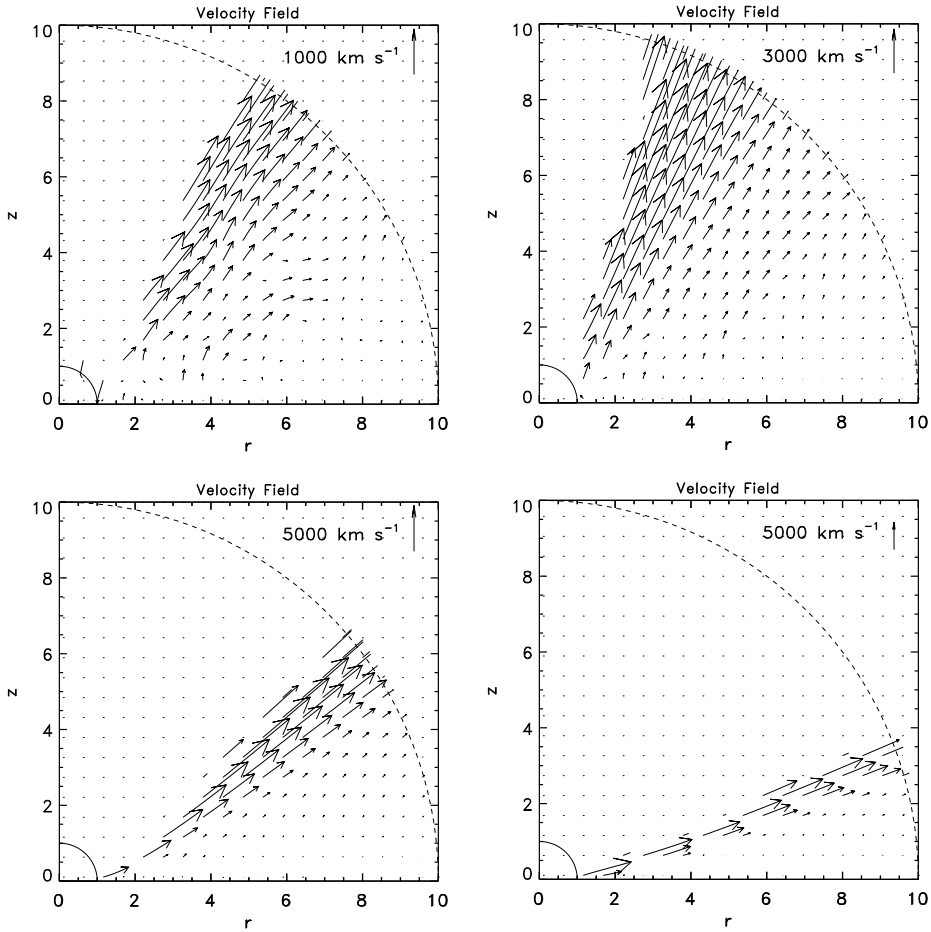


Figure 1. Maps of poloidal velocity for a range of LD disk wind models (Figure 2 in PSD 99). The top panels are both models with $x = 0$ but with $\dot{M}_a = 10^{-8} M_\odot \text{ yr}^{-1}$ (the left hand side panel) and $\dot{M}_a = \pi \times 10^{-8} M_\odot \text{ yr}^{-1}$ (the right hand side panel). The bottom two panels are results for models both with $\dot{M}_a = \pi \times 10^{-8} M_\odot \text{ yr}^{-1}$, but with $x = 1$ (the left hand side panel) and $x = 3$ (the right hand side panel). The top two panels show the effect on the outflow geometry of increasing the disk luminosity alone, while the top right and bottom two panels show the effect of adding in an increasingly larger stellar component ($x = 0, 1$ and 3) to the radiation field. Adding in an increasingly large stellar component causes the outflow to become more equatorial. Note that we suppress velocity vectors in regions of very low density (i.e., ρ less than $10^{-20} \text{ g cm}^{-3}$).

2.1. Nature of Unsteady Outflow

The fact that the unsteady behavior observed in PSD 98 models has not changed with a more accurate treatment of the radiation force indicates it is indeed a robust property of line driven winds from disks. Why does increasing the radial component of the radiation force 'organize' the wind into a steady state?

PSD 99, presented the following explanation; let r and z define position along a streamline in the wind in cylindrical coordinates. An increase of the

vertical component of the gravity, $g_z \propto -z/(r^2 + z^2)^{3/2}$ with height at a fixed radius r is the main driver of the unsteady flow. (We add that for a disk wind driven by the disk radiation is vertical and its density can decrease downstream only due to an increase in the velocity as there is no geometrical dilution.) The increase of the gravity with height can be significantly reduced if the streamlines are directed outwards from purely vertical (i.e., r increases with z). At the same time, this tilt also brings into play an increase of the horizontal effective gravity, g_r , along each streamline: $g_r \propto [r_f/r^3 - r/(r^2 + z^2)^{3/2}]$, where r_f is the radius on a Keplerian disk at which a streamline originates. However the increase of g_r with r' is slower than the increase of g_z with z' because of the decaying centrifugal term. In other words, the line force can more easily maintain domination over gravity if the flow climbs the gentler gravitational hill in the horizontal direction as compared with the vertical direction. Furthermore, driving material along streamlines outward from the vertical causes density to decline with radius due to geometrical dilution alone as r^{-p} with $p \approx 0.5 - 1.5$ — this, very usefully, tends towards increasing the line force, thereby facilitating a better match with trends in gravity.

We note that Proga, Stone, & Drew's discovery of unsteady flow in models for $x = 0$ has not been confirmed by Pereyra and his collaborators in their numerical simulations (Pereyra, Kallman, & Blondin 1997, 2000; Pereyra & Kallman 2003). Recently, Pereyra et al. (2004) presented mathematically simple models and used them to argue against the above explanation of unsteady nature of LD disk wind for $x = 0$. In particular, Pereyra et al. claimed that a gravitational force initially increasing along the wind streamline, which is characteristic of disk winds, does not imply an unsteady wind. However, we find that Pereyra et al. omitted the fact that the line force and consequently wind streamlines are coupled to the gravitational force and radiation field. We also note that Vitello & Shlosman (1988) studied analytically LD driven disk wind model where streamlines were vertical near the disk and diverging to spherical at large distances. Vitello & Shlosman found that for a steady state solution to exist it is necessary to enforce a radiation force term to increase with height. PSD 98 and PSD 99's results are then consistent with Vitello & Shlosman's result because for the case where the wind is vertical near the disk only unsteady solution exist (PSD 98 computed the radiation force self-consistently and did not enforce any special increase of it with height [See however Pereyra, Kallman, & Blondin (1997)]. In summary, we conclude Pereyra et al. 's mathematically simple models, if anything support PSD 98 and PSD 99's interpretation of unsteady winds: when one considers the radiation and flow geometry appropriate for the $x = 0$ case (i.e., radiation and flow are vertical near the disk) then analytic analysis similar to that used by Pereyra et al. shows that there is no critical point (using the terminology from analytic models of LD stellar winds as adopted by Pereyra et al. (2004)). However, significant central radiation (as in the $x > 0$ cases) makes a dynamical and geometrical change in the wind solution i.e., increases the wind inclination angle and a critical point can exist.

2.2. Testing Models Against Observations

Applying PSD 98 and PSD 99's dynamical models to CVs one finds that radiation driving can produce disk winds consistent with the following observed properties of CV winds: (i) the flow is biconical rather than equatorial as required by the absence of blueshifted line absorption from the spectra of eclipsing high-state CV, (ii) the wind terminal velocity is comparable to the escape velocity from the surface of the white dwarf (WD), and (iii) the spectral signatures of mass loss show a sharp cut-off as the total luminosity in dwarf novae declines away from maximum light through the regime theoretically identified as likely to be critical.

Additionally, LD disk wind models may explain the highly unsteady and continuously variable nature of the supersonic outflows in the NL binaries BZ Cam and V603 Aql (Prinja et al. 2000a,b). The presence of a slow, dense transition region between disk photosphere and outflow in V347 Pup and UX UMa (Shlosman, Vitello, & Mauche 1996; Knigge & Drew 1997) may also be accommodated within these same models.

Building upon these numerical models, one can compare the results of these models with the analytic results readily derived for spherically-symmetric winds (e.g., Proga 1999). This comparison shows the achievable disk-wind mass loss rates differ only from the well-known one-dimensional analytic values by a factor (of geometric origin) of order unity. A very similar conclusion was reached by Feldmeier & Shlosman (1999) who compared their analytic LD disk wind models the two-dimensional numerical simulations of PSD 98) and found an overall good agreement in the streamline shape, tilt angle, and mass-loss rate. These agreement between numerical models and analytic ones allow us to generalize beyond the limited set of models for which numerical results already exist.

For example, Drew & Proga (2000) compared mass loss rates predicted by the models with observational constraints (Figure 2). They concluded that either mass accretion rates in high-state CVs are higher than presently thought by a factor of 2-3 or that radiation pressure alone is not quite sufficient to drive the observed hypersonic flows. The difficulty in accounting for the mass loss rate in a pure LD disk wind model for CVs is simply a reflection of the fact that the CV luminosities just barely satisfy the basic requirement, i.e., $L_{\text{UV}} \lesssim 7 \times 10^{-4} L_{\text{Edd}}$. A very similar conclusion has been reached by Mauche & Raymond (2000) who analyzed observations of OY Carinae taken by the Extreme Ultraviolet Explorer. Mauche & Raymond argued that line driving alone falls an order of magnitude short of driving the observed mass-loss rate.

Generally, one can argue that in all accretion disks, with the UV luminosity, $L_{\text{UV}} \gtrsim$ a few $10^{-4} L_{\text{Edd}}$ mass outflows have been observed (Proga 2002). For example, accretion disks around: massive black holes, WDs (as in AGN and CVs with $L_{\text{UV}} \gtrsim 0.001 L_{\text{Edd}}$) and low mass YSOs (as in FU Ori stars with $L_{\text{UV}} \gtrsim$ a few $\times 0.01 L_{\text{Edd}}$) show powerful fast winds. Systems that have too low UV luminosities to drive a wind include accretion disks around neutron stars and low mass black holes as in low mass X-ray binaries and galactic black holes. These systems indeed do not show outflows similar to those observed in CVs, AGN and FU Ori.

Comparing the wind properties (e.g., \dot{M}_w and geometry) inferred from observations with the wind properties predicted by models for given systems pa-

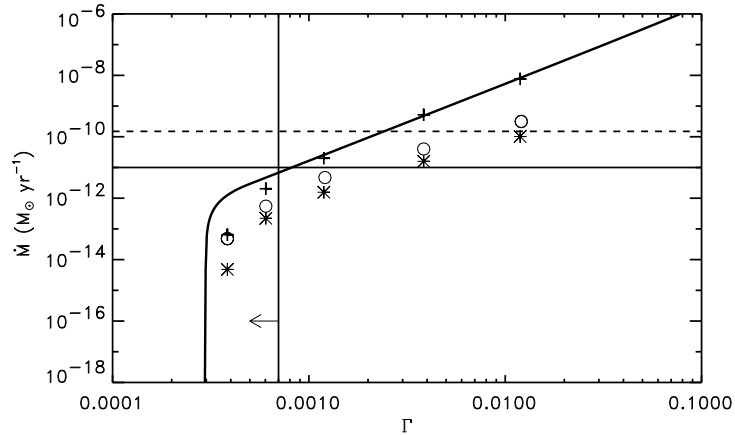


Figure 2. Model mass loss rates for radiation-driven disk winds as a function of Γ where $\Gamma \equiv L/L_{\text{Edd}}$ [Figure 1 in Drew & Proga (2000)]. The solid-line curve is the 1-dimensional mass loss rate, derived analytically, in the case that $M_{\text{max}} = 4000$ and $\alpha = 0.4$. Also shown are numerical disk-wind mass loss rates for the same M_{max} for $\alpha = 0.4$ (crosses), 0.6 (circles), 0.8 (asterisks). (See (Proga 1999) for further details). The vertical line superimposed is drawn at Γ corresponding to a mass accretion rate of $10^{-8} M_{\odot} \text{ yr}^{-1}$ onto a CO white dwarf of mass $1 M_{\odot}$ – presently mass accretion rates are believed to be less than this. The solid horizontal line typifies current $\dot{M} \xi_{C^{3+}}$ estimates, while the dashed line is the lower limiting mass loss rate construed from wind ionization models.

rameters is one way of testing the models. It would be very instructive to compute synthetic spectra based on the models and compare these with observed spectra. Such synthetic line profiles were computed by Proga et al. (2002) using a generalized version of the Sobolev approximation. In this study, the attention was restricted to the case of a representative UV transition of a light ion such as C IV or Si IV. The assumed abundance and atomic data were appropriate to the C IV $\lambda 1549$ treated as singlet.

Generally, Proga (2002) found that the two main wind components (slow wind and fast stream) produce distinct spectral features. The fast stream produces profiles which show features consistent with observations. These include the appearance of the classical P-Cygni shape for a range of inclinations, the location of the maximum depth of the absorption component at velocities less than the terminal velocity, and the transition from net absorption to net emission with increasing inclination. However the model profiles have too little absorption or emission equivalent width compared to observed profiles. This quantitative difference between the models and observations is not a surprise because, as we discussed above, the LD wind models predict a mass loss rate, mostly due to the fast stream, that is lower than the rate required by the observations.

A key parameter shaping the total line profile – made up of both scattered emission and absorption – is the ratio of the expansion velocity to the rotational velocity. This ratio is a cause of some differences in the line profile between models with or without radiation from the central star. For models with the WD radiation switched on (the bottom panels on Figure 3), the winds are less bipolar and so the rotational velocity decreases along the wind streamlines faster than

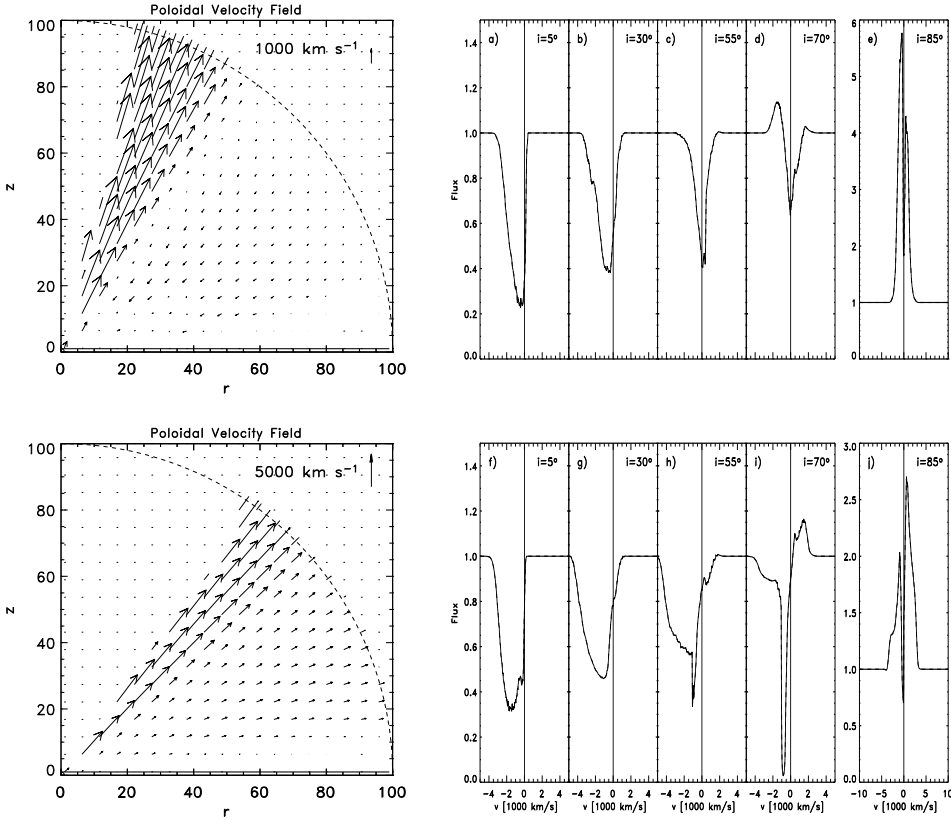


Figure 3. Maps of poloidal velocity (the left hand side column of panels) and line profiles (2-6 columns of panels) for two representative models of LD disk winds. The line profiles are shown for a range of inclination angles, i (see top right corner of each panel for the value of i). The top panels are for the wind model with $x = 0$ and $\dot{M}_a = \pi \times 10^{-8} M_\odot \text{ yr}^{-1}$ [B2 model in Proga (2003b)]. The bottom panels show results for the model with $\dot{M}_a = \pi \times 10^{-8} M_\odot \text{ yr}^{-1}$ and $x = 1$ [C2 model in Proga (2003b)]. The zero velocity corresponding to the line center is indicated by the vertical line in the panels shown line profiles. Note the difference in the velocity and flux ranges in the planes for $i = 85^\circ$ (the right hand side column).

for models with the WD radiation switched off (the top panels in Figure 3). This simple change in the wind geometry reduces the rotational velocity of the flow compared to the expansion velocity. The relatively higher expansion velocity has an important consequence on the scattered emission: for $x \gtrsim 1$ at high inclination ($i \gtrsim 60^\circ$), the red component of the scattered emission becomes stronger – stronger than the blue component of the emission and stronger than the blueshifted absorption so it is strong enough for the total line to have a P Cygni profile (e.g., Figure 3i).

In the follow up paper, we found that the inclusion of a disk wind at larger radii changes qualitatively and quantitatively the line profiles predicted by the LD disk wind model (Proga 2003b). The models computed on a small grid –

such as those in PSD 99, where the outer radius equals 10 WD radii – suffice to calculate the gross properties of the disk wind. For example, the radial range of 10 WD radii suffice to calculate \dot{M}_w and the fast part of the wind, which are both associated with the outflow from the innermost disk. However, such calculations do not capture the entire region where lines are formed. As a result, they underpredict the line absorption and to a lesser extent the scattered emission. The simulations on the small grid predicted a double-humped structure near the line center for intermediate inclinations (e.g., Proga 2002). This structure is due to a non-negligible red-shifted absorption that is formed in the slow wind where the rotational velocity dominates over expansion velocity.

In Proga (2003b), we showed that by taking into account the downstream part of the same slow wind one is able to increase significantly the central absorption. As a result, the double-humped structure is reshaped to a more typical broad trough. We emphasize that all improvements in the shape as well as the strength of the absorption were achieved without changing the gross properties of the wind. In particular, our new models do not predict a higher mass-loss rate than the previous models. The changes in the line profiles are mainly caused by the fact that the ratio between the rotational and poloidal velocity decreases downstream. Overall, one finds that the wind-formed line profiles seen at ultraviolet wavelengths cannot originate in a flow where rotation and poloidal expansion are comparable. The UV lines must trace gas that expands substantially faster than it rotates.

The main discrepancy between the predicted line profiles and the observed ones is in the line emission. Specifically, the model cannot produce the red-shifted emission as strong as that seen, for example, in the CIV profile of many systems with intermediate inclinations (see below). However, this shortcoming is not a great surprise – this has been a problem for a while (see e.g., Mauche, Lee, & Kallman 1997; Ko et al. 1996, and discussion below).

A systematic comparison between predicted line profiles and observations for many systems is a crucial test the idea that the LD disk wind model can work for CV winds in the sense that it can reproduce the observed line profiles for model parameters (e.g., L) suitable to CVs. Preliminary results from limited survey of dynamical models and their predictions are promising. For example, Figure 4 presents a comparison between profiles derived from the model with $M_a = \pi \times 10^{-8} M_\odot \text{ yr}^{-1}$, $x = 0.25$ [model E2 in Proga (2003b) for which $\dot{M}_w = 8 \times 10^{-8} M_\odot \text{ yr}^{-1}$] and observations of the CIV 1549Å transition of IX Vel (Hartley et al. 2002). [To show how much line emission is required, only the absorption component is plotted.] The observed i for this system is 60° (Beuermann & Thomas 1990).

Figure 4 shows that the model profiles well reproduce the blue-shifted absorption despite a relatively low \dot{M}_w . Thus the gap between the kinematics of the LD wind models and reality is narrower than comparison between observed and theoretical \dot{M}_w 's would indicate. The gap is only narrowed but not bridged yet because the mass fluxes required to match the observed spectra at least of IX Vel are somewhat higher than those observed. As Drew & Proga (2000) discussed, the luminosity of the system requires a mass accretion rate of at most $10^{-8} M_\odot \text{ yr}^{-1}$, whereas the line profiles require $M_a = \pi \times 10^{-8} M_\odot \text{ yr}^{-1}$ and $x = 0.25$, yielding a system luminosity higher than the observed one by a factor

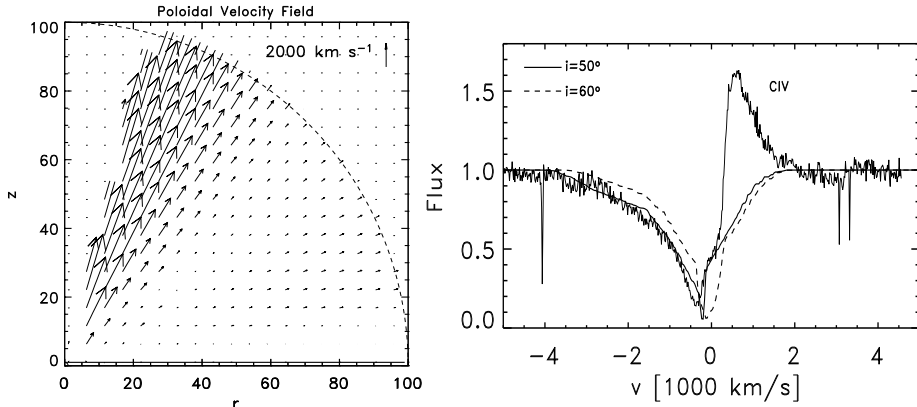


Figure 4. A map of poloidal velocity and line profiles. The right hand side panel, compares profiles derived from a wind model for $i = 50^\circ$ and 60° (thick solid and thick dashed line, respectively) and observations of the CIV 1549 Å in the spectrum of the brightest nova-like variable, IX Vel (Hartley et al. 2002). The synthesized lines show the absorption component without the contribution from the scattered emission (see the main text).

of ~ 4 . However, the main point here is that this discrepancy is much smaller than it used to be (i.e., it was more than 1 order of magnitude) and there is a good chance that it can be reduced still further.

For example, in Proga (2003b) we have computed many models, changing various model parameters such as \dot{M}_a and the parameters of the force multiplier, α and M_{\max} . In general, in Proga (2003b) found that there is a degeneracy in the model parameters as far as line profiles are concerned (PSD 98 found an analogous degeneracy for the wind properties). For example, models with slightly different parameters – such as \dot{M}_a and α – produce similar line profiles for different i . Additionally, a model with $\dot{M}_a = 10^{-8} M_\odot \text{ yr}^{-1}$ and $\alpha = 0.674$ predicts very similar line profiles to model with $\dot{M}_a = \pi \times 10^{-8} M_\odot \text{ yr}^{-1}$ and $\alpha = 0.6$ for the same i . Finally, we find that the product $(1+x)L_D M_{\max}$, not its individual factors, appears to be a fundamental parameter determining the line profiles (i.e., their width and depth) for the parameter range applicable to CVs. This has an important implication for LD models: to obtain a theoretical fit as good as shown in Figure 4 for a fixed i , one needs $(1+x)L_D M_{\max} \sim 1.3 \times 10^5 L_\odot$ rather than specifically $x = 0.25$, $M_{\max} = 4400$, and $L_D = 23.4 L_\odot$ as for the model shown in Figure 4.

The above mentioned successes of LD disk wind models are encouraging but there are also problems. For example, if radiation pressure powers the mass loss from CVs, the wind mass-loss rate should increase with increasing system luminosity (e.g., PSD 98; Proga1999).). However recent HST observations of IX Vel and V3885 Sgr showed that the wind spectral features do not correlate with the system luminosity (Hartley et al. 2002). If confirmed, these observations seriously challenge the pure LD disk wind scenario.

2.3. Limitations of LD models and future work

We conclude this section with a reminder of the limitations of the present LD disk wind models. Many of the details of the models depend on details of the assumptions about the disk and microphysics of the wind. For example, the assumed form for the background radiation field inevitably plays a role in the comparison of observed profiles with synthetic profiles based on any model, kinematic or dynamical. However for line fitting based on LD wind models, the adopted disk and WD radiation fields are even more important because they determine all wind properties except the initial Keplerian component of motion. Current models adopt the dependence of the disk radiation on radius according to the standard steady state disk model (e.g., Pringle 1981). This assumption is a good starting point but it should be remembered that actual disks may only be very crudely described by simple theory or they may yield unexpected features such as chromospheric emission. In fact, spectral synthesis models of accretion disk photospheres (e.g., Linnell & Hubeny 1996; Wade & Hubeny 1998; Wade & Orosz 1999) have typically failed to adequately reproduce observed energy distributions where direct comparisons have been made (see e.g., Long et al. 1994). There has been a similar lack of success in past calculations of accretion disk line emission. Specifically, the accounting for both the strengths of and the flux ratios among various emission lines in a large ensemble of observed CVs has not been compelling (Mauche, Lee, & Kallman 1997; Ko et al. 1996). These models either miss a crucial physical component or employ an inappropriate physical assumption which affects the predicted line emission. It is for this reason that, in comparing model wind profiles with observation, we concern ourselves more with the absorption component than with the emission.

In line profile calculations, Proga (2002) and Proga (2003b) assumed that the ionization fraction of scattering species is constant (ξ_{ion} is set to unity). A proper allowance for a variation of ξ_{ion} with position to values less than one can only serve to weaken the overall line profile. [Examples of plots of this potentially very marked positional dependence may be found in the work of Shlosman & Vitello (1993) and Long & Knigge (2002)]. Therefore, it is important to carry out time-dependent calculations of the wind photoionization structure. It is also important to perform simulations in fully three dimensions to explore nonaxisymmetric effects. The two photoionization and three dimensional effects are most likely coupled (e.g., by the wind density) and it would be essential to study them self-consistently.

3. MHD Models

One of the reasons for considering magnetic fields as an explanation for winds from accretion disks is the fact that magnetic fields are very likely crucial for the existence of all accretion disks. The magnetorotational instability (MRI) has been shown to be a very robust and universal mechanism to produce turbulence and the transport of angular momentum in disks at all radii (Balbus & Hawley 1991, 1998). It is therefore likely that magnetic fields control mass accretion inside the disk and play a role in producing a disk wind.

In fact, magnetically driven winds from disks are the favored explanation for the outflows in many astrophysical environments. Blandford & Payne

(1982) (see also Pelletier & Pudritz 1992) showed that the centrifugal force can drive a wind from the disk if the poloidal component of the magnetic field, \mathbf{B}_p makes an angle of $> 30^\circ$ with respect to the normal to the disk surface. Generally, centrifugally-driven MHD disk winds (magnetocentrifugal winds for short) require the presence of a sufficiently strong, large-scale, ordered magnetic field threading the disk with a poloidal component at least comparable to the toroidal magnetic field, $|B_\phi/B_p| \lesssim 1$ (e.g., Cannizzo & Pudritz 1989; Pelletier & Pudritz 1992). Several groups have studied numerically axisymmetric winds using the Blandford & Payne mechanism (e.g., Usyugova et al. 1995; Ouyed & Pudritz 1997a,b; Krasnopolksy, Li, & Blandford 1999; Kato, Kudoh & Shibata 2002). An important feature of magnetocentrifugal winds is that they require some assistance to flow freely and steadily from the surface of the disk, to pass through a slow magnetosonic surface (e.g., Blandford & Payne 1982). The numerical studies mentioned above do not resolve the vertical structure of the disk but treat it as a boundary surface through which mass is loaded on to the magnetic field lines at a specified rate.

Winds from disks can also be driven by the magnetic pressure. In particular, the toroidal magnetic field can quickly build up due to the differential rotation of the disk so that $|B_\phi/B_p| \gg 1$. In such a case, the magnetic pressure of the toroidal field can give rise to a self-starting wind (e.g., Uchida & Shibata 1985; Pudritz & Norman 1986; Stone & Norman 1994; Contopoulos 1995; Kudoh & Shibata 1997). To produce a steady outflow driven by the magnetic pressure a steady supply of advected toroidal magnetic flux at the wind base is needed, otherwise the outflow is likely to be transient (e.g., Königl 1993; Contopoulos 1995). It is still not clear whether the differential rotation of the disk can produce such a supply of the toroidal magnetic flux to match the escape of magnetic flux in the wind and even if it does whether such a system will be stable (e.g., Contopoulos 1995; Ouyed & Pudritz 1997b, and references therein).

To our best knowledge, in Proga (2003a), we were first to report on numerical simulations of the two-dimensional, time-dependent MHD structure of LD winds from luminous accretion disks initially threaded by a purely axial magnetic field. We developed self-consistent models of such winds and applied them to winds from CVs. Our models require less free parameters than previous MHD models. In particular, the model predicts the mass loss rate.

In Proga (2003a), we used ideal MHD to compute the evolution of Keplerian disks, varying the magnetic field strength and L_D , L_* , or both. We found that the magnetic field very quickly starts deviating from purely axial due to MRI. This leads to fast growth of the toroidal magnetic field as field lines wind up due to the disk rotation. As a result the toroidal field dominates over the poloidal field above the disk and the gradient of the former drives a slow and dense disk outflow, which conserves specific angular momentum of fluid.

Our LD-MHD simulations also showed that depending on the strength of the magnetic field relative to L the disk wind can be LD or MHD-driven. For very weak magnetic fields, similarly to the LD wind, the wind consists of a dense, slow outflow that is bounded on the polar side by a high-velocity stream. The mass-loss rate is mostly due to the fast stream. As the magnetic field strength increases first the slow part of the flow is affected, namely it becomes even denser and slightly faster and begins to dominate the mass-loss rate. In very strong

magnetic field or pure MHD cases, the wind consists of only a dense, slow outflow without the presence of the distinctive fast stream so typical of pure LD winds. Our simulations indicate that winds launched by the magnetic fields are likely to remain dominated by the fields downstream because of their relatively high densities. Line driving may not be able to change a dense MHD wind because the line force strongly decreases with increasing density.

The increase of the mass loss rate due to the MHD effects is a welcome development in modeling CV winds. However, it is unclear whether LD-MHD models can resolve the problem of too low \dot{M}_w . As we discussed in section 2, to explain CV winds we need a model that predicts not only a higher \dot{M}_w but also \dot{M}_w must be mostly due to a fast wind not a dense slow rotating wind as we found in our LD-MHD models.

3.1. Limitations of LD-MHD models and future work

The most important limitation of LD-MHD simulations is an inadequate spatial resolution for modeling the MRI inside the disk. These are only preliminary simulations we aimed to examine the parameter space of the models that will define the major trends in disk wind behavior. Therefore the priority has been so far to set up the simulations in such a way that the base of the wind is relatively stable and corresponds to a steady state accretion disk.

The fact that LD-MHD results strongly depend on the magnetic field points to a need to explore different configurations for the initial magnetic field and to move from two-dimensional axisymmetric simulations to fully three-dimensional simulations. It is important to follow the long-time evolution of the flow. Therefore three-dimensional simulations are required as there exist no self-sustained axisymmetric dynamos. Thus, contrary to the stellar winds, simulations of winds from magnetized disks – with or without radiation pressure – should include the disks themselves, not just the disk photosphere, and should be performed in three dimensions.

4. Conclusion

Our main conclusion is that, despite some problems, line-driving alone is still the most plausible mechanism for driving the CV winds. Preliminary results from LD-MHD wind models confirm that magnetic driving is likely an important element of the wind dynamics. However, magnetic driving does not seem to be necessary to produce a wind. The most important issues which need to be addressed by future dynamical models, regardless of driving mechanism, are the effects of the position-dependent photoionization and the dynamical effects in three dimensions.

Acknowledgments. We acknowledge support from NASA under LTSA grant NAG5-11736. We also acknowledge support provided by NASA through grant AR-09947 from the Space Telescope Science Institute, which is operated by the Association of Universities for Research in Astronomy, Inc., under NASA contract NAS5-26555.

References

Balbus, S.A., & Hawley, J.F. 1991, *ApJ*, 376, 214

Balbus, S.A., & Hawley, J.F. 1998, *Rev. Mod. Phys.*, 70, 1

Beuermann, K., & Thomas, H.-C. 1990, *A&A*, 230, 326

Blandford, R.D., & Payne, D.G. 1982, *MNRAS*, 199, 883

Cannizzo, J.K., & Pudritz, R.E. 1988, *ApJ*, 327, 840

Contopoulos, J. 1995, *ApJ*, 450, 616

Castor, J.I., Abbott, D.C., & Klein, R.I. 1975, *ApJ*, 195, 157 (CAK)

Drew, J.E. 1987, *MNRAS*, 224, 595

Drew, J.E., & Proga, D. 2000, in *Cataclysmic Variables*, Symp. in Honour of Brian Warner, ed. P. Charles et al. (Amsterdam: Elsevier), 21

Feldmeier, A., & Shlosman, I. 1999, *ApJ*, 526, 344

Friend, D.B., & Abbott, D.C. 1986, *ApJ*, 311, 701

Hartley, L.E., Drew, J.E., Long, K.S., Knigge, C., & Proga, D. 2002, *MNRAS*, 332, 127

Kato, S.X., Kudoh, T., & Shibata, K. 2002, *ApJ*, 565, 1035

Knigge, C., Drew, J.E. 1997, *ApJ*, 486, 445

Knigge, C., Woods, J.A., & Drew, J.E. 1995, *MNRAS*, 273, 225

Ko, Y., Lee, P.Y., Schlegel, E.M., & Kallman, T. R. 1996, *ApJ*, 457, 363

Königl A. 1993, in *"Astrophysical Jets"*, ed. D.P. O'Dea (Cambridge: CUP), 239

Krasnopolsky, R., Li, Z.-Y., & Blandford, R. 1999, *ApJ*, 526, 631

Kudoh, T., & Shibata, K. 1997, *ApJ*, 474, 362

Linnell, A.P., & Hubeny, I. 1996, *ApJ*, 471, 958

Long, K.S., & Knigge, C. 2002, *ApJ*, 579, 725

Long, K.S., Wade, R.A., Blair, W.P., Davidsen, A.F., & Hubeny, I. 1994, *ApJ*, 426, 704

Mauche, C.W., Lee, Y.P., & Kallman, T.R. 1997, *ApJ*, 477, 832

Mauche, C.W., & Raymond, J.C. 1987, *ApJ*, 323, 690

Mauche, C.W., & Raymond, J.C. 2000, *ApJ*, 323, 690

Murray, N., Chiang, J., Grossman, S.A., & Voit, G.M. 1995, *ApJ*, 451, 498

Ouyed, R., & Pudritz, R.E. 1997a, *ApJ*, 482, 717

Ouyed, R., & Pudritz, R.E. 1997b, *ApJ*, 484, 794

Pauldrach, A., Puls, J., & Kudritzki, R.P. 1986, *A&A*, 164, 86

Pelletier, G., & Pudritz, R.E. 1992, *ApJ*, 394, 117

Pereyra, N.A., Kallman, T.R., & Blondin, J.M. 1997, *ApJ*, 477, 368

Pereyra, N.A., Kallman, T.R., & Blondin, J.M. 2000, *ApJ*, 532, 563

Pereyra, N.A., & Kallman, T.R. 2003, *ApJ*, 582, 984

Pereyra, N.A., Owocki, S.P., Hillier, D.J., & Turnshek, D.A. 2004, *ApJ*, 608, 454

Pringle, J.E. 1981, *ARAA*, 19, 137

Prinja, R.K., Knigge, C., Ringwald, F.A., & Wade, R.A. 2000, *MNRAS*, 318, 368, b

Prinja, R.K., Ringwald, F.A., Wade, R.A., & Knigge, C. 2000, *MNRAS*, 312, 316, a

Proga, D. 1999, *MNRAS*, 304, 938

Proga, D. 2002, in *Mass Outflow in Active Galactic Nuclei: New Perspectives*, ASP Conf. Proc. Vol. 255, ed. D.M. Crenshaw, S.B. Kraemer, & I.M. George (San Francisco: ASP), 309

Proga, D., Kallman, T.R., Drew, J.E., & Hartley, L.E. 2002, *ApJ*, 572, 382

Proga, D. 2003, *ApJ*, 585, 406

Proga, D. 2003, *ApJ*, 592, L9

Proga, D., Stone, J.M., & Drew, J.E. 1998, *MNRAS*, 295, 595 (PSD 98)

Proga, D., Stone, J.M., & Drew, J.E. 1999, *MNRAS*, 310, 476 (PSD 99)

Pudritz, R.E., & Norman, C.A. 1986, *ApJ*, 301, 571

Shlosman, I., & Vitello, P.A.J. 1993, *ApJ*, 409, 372

Shlosman, I., Vitello, P.A.J., & Mauche, C.W. 1996, *ApJ*, 461, 377

Stone, J.M., & Norman, M.L. 1992, *ApJS*, 80, 753

Stone, J.M., & Norman, M.L. 1994, *ApJ*, 433, 746

Uchida, Y., & Shibata, K. 1985, *PASJ*, 37, 515

Ustyugova, G.V., Koldoba, A.V., Romanova, M.M., Chechetkin, V.M., & Lovelace, R.V.E. 1995, ApJ, 439, 39L
Vitello, P.A.J., & Shlosman, I. 1988, ApJ, 327, 680
Wade, R.A., & Hubeny, I. 1998, ApJ, 509, 350
Wade, R.A., & Orosz, J.A. 1999, ApJ, 525, 915